

# Antitumor Activity of PR-171, a Novel Irreversible Inhibitor of the Proteasome

Susan D. Demo, Christopher J. Kirk, Monette A. Aujay, Tonia J. Buchholz, Maya Dajee, Mark N. Ho, Jing Jiang, Guy J. Laidig, Evan R. Lewis, Francesco Parlati, Kevin D. Shenk, Mark S. Smyth, Congcong M. Sun, Marcy K. Vallone, Tina M. Woo, Christopher J. Molineaux, and Mark K. Bennett

Proteolix, Inc., South San Francisco, California

## Abstract

**Clinical studies with bortezomib have validated the proteasome as a therapeutic target for the treatment of multiple myeloma and non-Hodgkin's lymphoma. However, significant toxicities have restricted the intensity of bortezomib dosing. Here we describe the antitumor activity of PR-171, a novel epoxyketone-based irreversible proteasome inhibitor that is currently in clinical development. In comparison to bortezomib, PR-171 exhibits equal potency but greater selectivity for the chymotrypsin-like activity of the proteasome. In cell culture, PR-171 is more cytotoxic than bortezomib following brief treatments that mimic the *in vivo* pharmacokinetics of both molecules. Hematologic tumor cells exhibit the greatest sensitivity to brief exposure, whereas solid tumor cells and nontransformed cell types are less sensitive to such treatments. Cellular consequences of PR-171 treatment include the accumulation of proteasome substrates and induction of cell cycle arrest and/or apoptosis. Administration of PR-171 to animals results in the dose-dependent inhibition of the chymotrypsin-like proteasome activity in all tissues examined with the exception of the brain. PR-171 is well tolerated when administered for either 2 or 5 consecutive days at doses resulting in >80% proteasome inhibition in blood and most tissues. In human tumor xenograft models, PR-171 mediates an antitumor response that is both dose and schedule dependent. The antitumor efficacy of PR-171 delivered on 2 consecutive days is stronger than that of bortezomib administered on its clinical dosing schedule. These studies show the tolerability, efficacy, and dosing flexibility of PR-171 and provide validation for the clinical testing of PR-171 in the treatment of hematologic malignancies using dose-intensive schedules. [Cancer Res 2007;67(13):6383–91]**

## Introduction

The proteasome is a multicatalytic protease complex that is responsible for the ubiquitin-dependent turnover of cellular proteins (1–3). Proteasome substrates include misfolded or misassembled proteins as well as short-lived components of signaling cascades that regulate cell proliferation and survival pathways. Inhibition of the proteasome results in the accumulation of these substrate proteins and leads to cell death (4). The catalytic

core of the proteasome includes three proteolytic activities that are commonly described by their substrate selectivities (5): chymotrypsin-like, trypsin-like, and caspase-like. Each proteasome active site uses the side chain hydroxyl group of an NH<sub>2</sub>-terminal threonine as the catalytic nucleophile, a mechanism that distinguishes the proteasome from other cellular proteases (3).

Clinical validation of the proteasome as a therapeutic target in oncology has been provided by the dipeptide boronic acid bortezomib (also known as PS-341 or Velcade; refs. 4, 6). Bortezomib is a covalent, slowly reversible inhibitor that primarily targets the chymotrypsin-like activity of the proteasome (7). Bortezomib has proven efficacious as a single agent in multiple myeloma (8) and some forms of non-Hodgkin's lymphoma (NHL; refs. 9, 10). The cellular mechanism(s) responsible for the clinical efficacy of bortezomib remain unclear, but may include disruption of cell adhesion- and cytokine-dependent survival pathways, in part through suppression of NF- $\kappa$ B activity (11, 12), inhibition of angiogenesis (13), and/or activation of a misfolded protein stress response (14, 15). Although the clinical success of bortezomib is encouraging, a significant fraction of patients remain refractory to treatment (8–10). Furthermore, a number of toxicities including painful peripheral neuropathy (16) and thrombocytopenia (17) have restricted bortezomib to a biweekly day 1/day 4 dosing schedule that allows full recovery of proteasome activity between doses (18, 19). Therefore, clinical evaluation of additional proteasome inhibitor classes is warranted. Two irreversible proteasome inhibitors are currently under development: (a) salinosporamide A (NPI-0052), a natural product related to lactacyctin (20–22) and (b) PR-171, a modified peptide related to the natural product epoxomicin.

Epoxomicin was identified based on its *in vivo* antitumor activity (23) and subsequently shown to be a potent and selective inhibitor of the proteasome (24). Epoxomicin and its analogues are comprised of two key elements: a peptide portion that selectively binds in the substrate binding pocket(s) of the proteasome with high affinity and an epoxyketone pharmacophore that stereospecifically interacts with the catalytic threonine residue to irreversibly inhibit enzyme activity. X-ray crystallography has shown that epoxomicin forms a dual covalent morpholino adduct with the proteasome that requires the close juxtaposition of both the side chain hydroxyl and  $\alpha$ -amino groups of the active site threonine residue (25). This unique mechanism imparts a high degree of specificity to the proteasome relative to the active sites of other protease classes.

Medicinal chemistry efforts focused on increasing the potency and chymotrypsin-like selectivity of epoxomicin resulted in the identification of YU-101 (26), a synthetic tetrapeptide epoxyketone analogue. PR-171, a derivative of YU-101 with improved pharmaceutical properties, is currently under evaluation in phase I clinical

**Note:** Supplementary data for this article are available at Cancer Research Online (<http://cancerres.aacrjournals.org/>).

S.D. Demo and C.J. Kirk contributed equally to this work.

**Requests for reprints:** Mark K. Bennett, Proteolix, Inc., South San Francisco, CA 94080. E-mail: [mkbennett@proteolix.com](mailto:mkbennett@proteolix.com).

©2007 American Association for Cancer Research.

doi:10.1158/0008-5472.CAN-06-4086

trials in multiple myeloma and NHL. In the present study, we describe the *in vitro* characterization and preclinical pharmacology of PR-171. We show that PR-171 is a potent and selective inhibitor of the chymotrypsin-like activity of the proteasome, both *in vitro* and *in vivo*. In addition, we show that proteasome inhibition by PR-171 promotes apoptosis in a variety of tumor cell lines, and that daily dosing schedules that induce high levels of proteasome inhibition *in vivo* are well tolerated and result in antitumor activity in several xenograft models.

## Materials and Methods

**Materials.** PR-171 was synthesized as described by Smyth and Laidig (27). [<sup>3</sup>H]-PR-171 was generated by Pd-catalyzed tritiation of a 2-Br-Phe analogue of PR-171. Bortezomib was purchased from a local pharmacy. PR-171 and bortezomib stock solutions were prepared in DMSO and were diluted 100-fold for 20S proteasome assays or 400-fold for cell treatments. 7-Amino-4-methylcoumarin (AMC)-conjugated fluorogenic proteasome substrates were acquired from Boston Biochem (succinyl-Leu-Leu-Val-Tyr-AMC and Z-Leu-Leu-Glu-AMC) or Biomol (Boc-Leu-Arg-Arg-AMC and Z-Val-Gly-Arg-AMC). Purified human 20S proteasome, 20S immunoproteasome, and clasto-lactacystin  $\beta$ -lactone were purchased from Boston Biochem. Tissue culture media and horse serum were from Mediatech and fetal bovine serum (FBS) was from HyClone. Primary antibodies recognizing the following proteins were purchased from commercial sources:  $\beta$ -catenin, p21, cyclin B1, hsp27 phospho-Ser<sup>82</sup>, and actin from Cell Signaling Technology; ubiquitin from Biomol; and hsp27 and hsp70 from Abcam. Horseradish peroxidase (HRP)-conjugated secondary antibodies were acquired from Biosource.

**Cell lines.** Tumor cell lines were obtained from the American Tissue Culture Collection and were cultured in media recommended by the supplier. Nontransformed human umbilical vascular endothelial cells (HUVEC) and normal human dermal fibroblasts (NHDF) and their culture media [endothelial cell medium-2 (EGM-2) and fibroblast growth medium-1 (FGM-2), respectively] were obtained from Cambrex. All cells were maintained at 37°C in 5% CO<sub>2</sub>.

**Animals.** Male Sprague-Dawley rats (200–250 g) and female BALB/c (7–9 weeks old) and BNX (5–7 weeks old) mice were purchased from Charles River Laboratories and housed for 1 week before experimentation. For all experiments, animals had access to food and water *ad libitum*. All experiments were done under protocols approved by an institutional animal care and use committee.

**20S proteasome assays.** Proteasome chymotrypsin-like, caspase-like, and trypsin-like activities were determined using succinyl-Leu-Leu-Val-Tyr-AMC (10  $\mu$ mol/L), Z-Leu-Leu-Glu-AMC (10  $\mu$ mol/L), and Boc-Leu-Arg-Arg-AMC (50  $\mu$ mol/L), respectively, with purified human 20S proteasome (2, 4, and 8.0 nmol/L, respectively) or HT-29 cell lysate (0.125, 0.25, and 0.25  $\mu$ g protein/mL, respectively). Assay buffer consisted of TE buffer [20 mmol/L Tris (pH 8.0), 0.5 mmol/L EDTA] with (20S) or without (cell lysate) 0.03% SDS. Reactions were initiated by enzyme or lysate addition and monitored for AMC product formation at 27°C with a plate-based spectrofluorometer (Tecan). IC<sub>50</sub> values were determined based on the reaction velocity measured between 60 and 75 min. To evaluate the kinetics of proteasome inhibition, first-order rate constants ( $k_{obs}$ ) were derived from reaction progress curves for each inhibitor concentration.  $k_{inact}/K_i$  values were then determined from the slopes of the double reciprocal plot of  $1/k_{obs}$  versus  $1/[inhibitor]$  according to the equation  $1/k_{obs} = 1/k_{inact} + K_i/k_{inact} (1/[inhibitor])$ .

**Cell viability and cellular proteasome activity assays.** Drug treatments were done in RPMI 1640 containing 5% FBS, 100 units/mL penicillin, and 100  $\mu$ g/mL streptomycin (transformed cell lines), FGM-2 (NHDF) or EGM-2 (HUVEC). Cells were exposed to compounds or 0.25% DMSO at 37°C either continuously for 72 h or for a 1-h period followed by three washes with media (RPMI 1640 containing 5% FBS) and incubation for an additional 72 h. Cell viability was assessed using the CellTiter-Glo reagent (Promega). For cellular proteasome activity assays, cell lysates were prepared by hypotonic lysis either immediately following the 1-h drug

treatment or after the washout and incubation at 37°C for an additional 4, 24, or 72 h. Fluorogenic peptide substrates were mixed with the lysates and proteasome activities determined by the initial rate (first 10 min) of AMC product formation. For proteasome activity recovery studies, background was subtracted based on the slope of fully inhibited samples, and the rates were normalized to the number of viable cells in each sample as determined by the CellTiter-Glo assay.

**Apoptosis assays.** Tumor cell lines were treated with either PR-171, bortezomib, or 0.25% DMSO for 1 h followed by a washout as described above. RPMI 8226 and HS-Sultan cells were treated with 500 nmol/L drug, whereas HT-29 cells were treated with 2  $\mu$ mol/L drug. Cells were collected at 24 h (all cell types) and 72 h (HT-29 only) posttreatment. For measurement of apoptosis, cells were stained for surface annexin V and propidium iodide permeability using the BD Bioscience Apoptosis kit and the percentage of annexin V-positive cells was determined by flow cytometry. Induction of effector caspase activity (caspase 3/7) was evaluated in HS-Sultan cells exposed to a range of PR-171 concentrations for 1 h followed by a 5-h washout period. Caspase 3/7 activity was determined by Z-DEVD-R100 substrate cleavage with the Apo-ONE assay kit (Promega).

**Western blot analysis.** RPMI 8226 cells were treated for 1 h at 37°C with either 500 nmol/L PR-171, 500 nmol/L bortezomib, or 0.25% DMSO. HT-29 cells were treated for 1 h at 37°C with either 2  $\mu$ mol/L PR-171, 2  $\mu$ mol/L bortezomib, or 0.25% DMSO. After compound treatment, the cells were washed twice with media as described above and incubated at 37°C for an additional 4 or 24 h. The cells were then washed in PBS and lysed in PBS containing 0.2% TX-100 and protease inhibitor cocktail (Roche). Lysate proteins were resolved on NuPage gels (Invitrogen), transferred to nitrocellulose, and probed with the indicated antibodies. Immunoreactive bands were revealed by HRP-conjugated secondary antibody staining followed by chemiluminescence detection (Pierce).

**Pharmacokinetics and pharmacodynamics.** For pharmacokinetic analysis, PR-171 was given to rats ( $n = 4$  per dose group) as an i.v. bolus (1 mL/kg) at 2, 4.5, and 9 mg/kg in a solution containing 5% (w/v) hydroxypropyl- $\beta$ -cyclodextrin (Roquette) and 50 mmol/L sodium citrate (pH 3.5). Blood samples were collected at 2, 5, 10, 15, 30, 60, and 120 min postdose, and plasma PR-171 concentrations were measured in duplicate by LC/MS-MS. Pharmacokinetic analyses were done using WinNonlin (Pharsight Corp.). For pharmacodynamic studies, PR-171 was formulated in an aqueous solution of 10% (w/v) sulfobutylether- $\beta$ -cyclodextrin (Cydex) and 10 mmol/L sodium citrate (pH 3.5) for administration to rats (0.1–9 mg/kg) and mice (5–10 mg/kg). Bortezomib was formulated in saline containing 10 mg/mL mannitol for administration to mice at 1 mg/kg. At selected time points after i.v. drug administration, tissue samples (adrenal, brain, heart, liver, lung, and tumors) were collected and frozen at  $-80^{\circ}\text{C}$ . After thawing, tissue samples were homogenized in two volumes of lysis buffer. Whole blood was collected by cardiac puncture into tubes containing sodium heparin. Rat splenocytes (isolated by mechanical disruption) and bone marrow (flushed from the tibia) were washed with PBS and depleted of erythrocytes by hypotonic lysis (BD Pharmalyse; BD Pharmingen). Whole blood, splenocytes, and bone marrow cells were washed twice with PBS and then lysed in lysis buffer and frozen at  $-80^{\circ}\text{C}$ . Tissue homogenates and cell lysates were cleared by centrifugation, and supernatants were collected for protein quantitation and proteasome activity determination using fluorogenic peptide substrates as described above.

**Quantitative whole body autoradiography.** Radiolabeled [<sup>3</sup>H]-PR-171 (250  $\mu$ Ci per animal) was given as an i.v. bolus to rats at a total dose of 2 mg/kg. Animals were sacrificed 0.5 h postdose and underwent whole-body perfusion with saline before being frozen. Sections were taken to identify organs of interest, and radioactivity levels in tissues were calculated using the AIS software (Imaging Research Corp.). These studies were done at Covance Laboratories.

**Xenograft studies.** Tumors were established by s.c. injection of cell lines (passage number <9 and viability >95% at the time of implantation) in the right flank of BNX mice ( $n = 7$  per group). For HT-29 and RL studies, cell suspensions containing  $5 \times 10^6$  and  $1 \times 10^7$  cells, respectively, in a volume

of 0.1 mL were injected. Mice were randomized into treatment groups and dosing initiated when tumors reached  $\sim 50 \text{ mm}^3$  (HT-29) or  $\sim 90 \text{ mm}^3$  (RL). For the HS-Sultan model, 0.2 mL containing  $1 \times 10^7$  cells in a 1:1 mixture with Matrigel (BD Discovery Labware) was injected. Tumor volume was measured 1 day after implantation, and mice were randomized to treatment groups and dosing initiated when the average tumor size exceeded the average size on Day 1 by  $\sim 100 \text{ mm}^3$ . PR-171 and bortezomib were given as described above for pharmacodynamic studies. In all treatment groups, tumors were measured thrice weekly by recording the longest perpendicular diameters and tumor volumes were calculated using the equation  $V$  (in  $\text{mm}^3$ ) = (length  $\times$  width<sup>2</sup>)/2.

**Statistical analysis.** For comparisons of treatment groups, a one-way ANOVA followed by Bonferroni post hoc analysis using GraphPad Prism Software (version 4.01) was done. Statistical significance was achieved when  $P < 0.05$ .

## Results and Discussion

**PR-171 selectively inhibits proteasome chymotrypsin-like activity.** The peptide epoxyketone YU-101 is a potent and selective inhibitor of the chymotrypsin-like activity of the 20S proteasome (26). However, the low aqueous solubility of this compound ( $<1 \mu\text{g/mL}$ ) limits its utility *in vivo*. PR-171 is an analogue of YU-101 that exhibits improved aqueous solubility ( $>1000$ -fold) due to the introduction of an  $\text{NH}_2$ -terminal morpholino moiety (Fig. 1A). To evaluate the potency and selectivity of PR-171 for the three proteasome catalytic active sites, we monitored the rates of fluorogenic peptide substrate hydrolysis either by purified 20S proteasome or in a cell lysate. Like YU-101, PR-171 is potent and highly selective for the inhibition of the chymotrypsin-like activity of the proteasome (Table 1). PR-171 also inhibited the chymotrypsin-like activity of the immunoproteasome ( $\text{IC}_{50}$ , 33 nmol/L), an IFN- $\gamma$ -inducible form of the proteasome (28). The ability of PR-171 to inhibit the proteasome in intact cells was also examined (Fig. 1B). Incubation of HT-29 colorectal adenocarcinoma cells with PR-171 for 1 h resulted in a dose-dependent inhibition of all three proteasome catalytic activities with the chymotrypsin-like activity exhibiting the greatest sensitivity ( $\text{IC}_{50}$ , 9 nmol/L). The caspase-like and trypsin-like activities were inhibited to a greater extent in the cellular assay ( $\text{IC}_{50}$  values, 150–200 nmol/L) than in the isolated enzyme assay ( $\text{IC}_{50}$  values,  $>1 \mu\text{mol/L}$ ; Table 1). Whether this reflects differences in the proteasome (e.g., 26S versus 20S) or cellular environment (e.g., accumulation) remains to be determined. Similar dose-dependent suppression of proteasome activity was observed in other cell lines with PR-171 (data not shown).

Although PR-171, bortezomib, and salinosporamide A exhibit comparable potency on the proteasome chymotrypsin-like activity, bortezomib and salinosporamide A inhibit the caspase-like and trypsin-like activities, respectively, with greater potency than PR-171 (Table 1, Fig. 1B; refs. 20, 22). As a result, bortezomib and salinosporamide A may have a greater impact on overall protein turnover (29). Mechanistically, the epoxyketone pharmacophore of PR-171 is more selective for the unique  $\text{NH}_2$ -terminal threonine active site of the proteasome than either the boronic acid of bortezomib or the  $\beta$ -lactone of salinosporamide A (3). Both bortezomib and salinosporamide A have been shown to inhibit certain serine proteases with micromolar or submicromolar potencies (7, 20). In contrast, neither epoxomicin (24) nor PR-171<sup>1</sup> has significant activity

on other protease classes at concentrations up to  $10 \mu\text{mol/L}$ . The selectivity of PR-171 for the chymotrypsin-like activity of the proteasome as well as its weak activity on other protease classes may contribute to greater tolerability *in vivo* (see below).

**Cellular proteasome activity recovers following PR-171 treatment.** Although both PR-171 and bortezomib form covalent adducts with the proteasome (25, 30), the hydrolytic stability of the two inhibitor-enzyme complexes differ: the dual covalent morpholino adduct formed with PR-171 is irreversible, whereas the tetrahedral intermediate formed with bortezomib is slowly reversible (3). To evaluate the impact of this difference on the kinetics of proteasome activity recovery in cells, chymotrypsin-like activity was monitored over the course of 72 h following inhibitor treatment (Fig. 1C). Despite the irreversible binding of PR-171 to the proteasome, the rate of recovery of proteasome activity in cultured cells ( $t_{1/2} \sim 24$  h) was only moderately slower than that observed with bortezomib. These results suggest that with both compounds, recovery of proteasome activity is due primarily to induction of mRNA transcription and *de novo* proteasome synthesis (31, 32).

**Brief exposure to PR-171 induces apoptosis and growth arrest in tumor cell lines.** The cytotoxic and proapoptotic effects of proteasome inhibitors are well established (3, 4, 10, 20, 33). However, most studies assessing the impact of proteasome inhibition on cells in culture have used extended treatment periods (24–72 h) that do not reflect the *in vivo* exposure that is achieved with either bortezomib or PR-171 due to their rapid clearance from plasma (see below and ref. 19). Therefore, we evaluated the cytotoxic effects of PR-171 and bortezomib on a panel of tumor cell lines and nontransformed cells treated for 1 h followed by a 72-h washout period (Table 2). Following brief exposure, PR-171 was more cytotoxic than bortezomib regardless of cell type, and both compounds were generally more cytotoxic to hematologic tumor lines than either solid tumor lines or nontransformed cells. No differences have been observed between PR-171 and bortezomib with regard to the onset of proteasome inhibition in a number of cell lines,<sup>1</sup> eliminating the possibility that differences in cell penetration or proteasome accessibility are responsible for these observations. It is possible that the somewhat slower rate of proteasome activity recovery following PR-171 treatment results in greater cytotoxicity.

To evaluate the mechanisms underlying the cytotoxic effects of PR-171, the impact of brief compound exposure on the induction of apoptosis and growth arrest in tumor cells was examined. Following treatment with PR-171 for 1 h, apoptosis was rapidly induced in the two hematologic tumor cell lines (RPMI 8226 and HS-Sultan) with maximum annexin V staining detected by 24 h (Fig. 2A) and effector caspase activation detected as early as 5 h (Fig. 2B). In contrast, HT-29 cells initially growth arrest at 24 h, with an accumulation of cells in the  $G_2$ -M and S phases of the cell cycle (Supplementary Fig. S1) and only later undergo apoptosis (by 72 h). Brief treatments with PR-171 were more effective than equivalent concentrations of bortezomib at promoting both apoptosis and growth arrest.

**Brief exposure to PR-171 promotes accumulation of proteasome substrates and markers of apoptosis or stress response pathways.** To further investigate the pathways activated by PR-171, Western blot analysis was done on cell lysates prepared from either RPMI 8226 (Fig. 2C) or HT-29 cells (Fig. 2D) either 4 or 24 h after a 1-h treatment with compound. The markers examined included direct proteasome substrates as well as markers that

<sup>1</sup> S.D. Demo, M.A. Aujay, T.J. Buchholz, F. Parlati, M.K. Vallone, T.M. Woo, M.K. Bennett, unpublished observation.

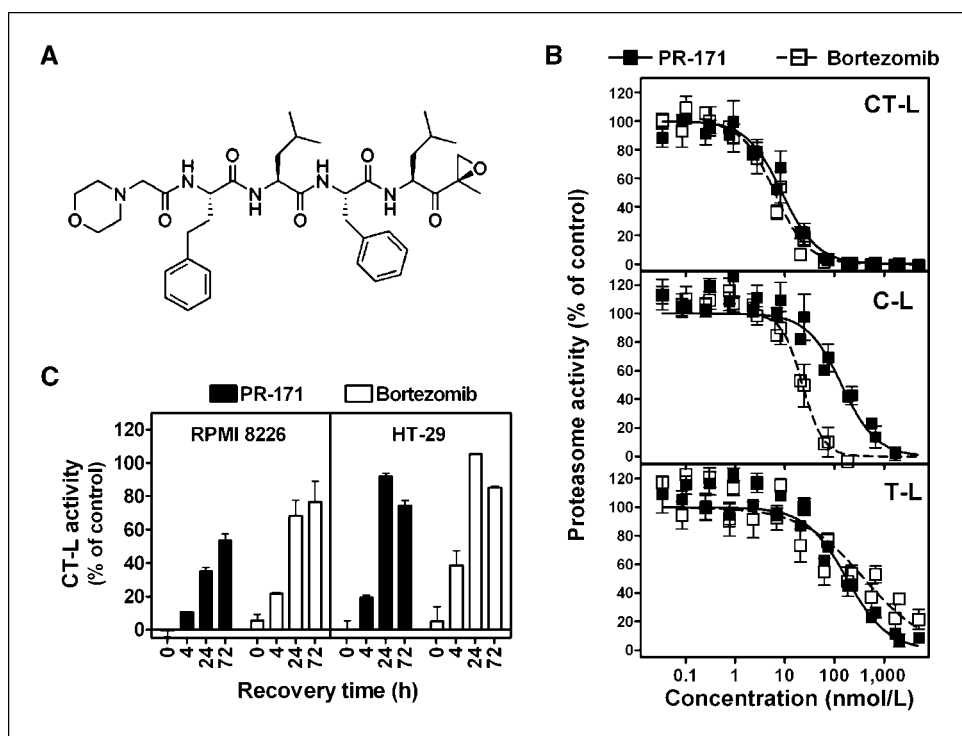


**Figure 1.** Inhibition and recovery of proteasome activity in tumor cell lines. **A**, structure of the epoxomicin analogue PR-171. **B**, active site selectivity of PR-171 and bortezomib in HT-29 cells. HT-29 cells were treated with PR-171 (■) or bortezomib (□) for 1 h and the proteasome chymotrypsin-like (CT-L), caspase-like (C-L), and trypsin-like (T-L) activities were measured in cell lysates with Leu-Leu-Val-Tyr-AMC, Leu-Leu-Glu-AMC, and Leu-Arg-Arg-AMC, respectively. Points, mean from  $\geq 3$  measurements presented as the percent activity relative to vehicle treated cells; bars, SE. **C**, recovery of cellular proteasome activity following PR-171 or bortezomib exposure. Proteasome chymotrypsin-like activity was measured in lysates prepared from RPMI 8226 (left) and HT-29 cells (right) at the indicated times following exposure to 32 nmol/L PR-171 (solid columns) or 32 nmol/L bortezomib (open columns) for 1 h. Columns, mean rate of fluorogenic Leu-Leu-Val-Tyr-AMC substrate hydrolysis presented as the percent activity relative to vehicle-treated cells; bars, SE.

accumulate as a functional consequence of activation of apoptotic, growth arrest, or stress response pathways. Each of the markers has been previously shown to accumulate in cells treated for extended periods with proteasome inhibitors (12, 31, 33–37). The effects of proteasome inhibition on the different markers varied by drug, cell line, and time point of analysis. Although accumulation of polyubiquitin chains was observed in both cell types within 4 h, the accumulation of other proteasome substrates was cell type specific, e.g., cyclin B1 in HT-29 and  $\beta$ -catenin in RPMI 8226. Although p21 levels increased in both cell types, the effect was more rapid in RPMI 8226 cells. The effects of PR-171 on accumulation of these markers was more pronounced than with bortezomib, consistent with the greater effects of brief PR-171 exposure on cell viability, apoptosis, and cell cycle progression. Heat shock protein induction is a common response to cellular stress, including perturbation of proteasome function and accumulation of misfolded proteins (31, 36, 38, 39). Both hsp27 and hsp70 were elevated at the 24-h time point in both cell lines and with both drugs, suggesting that this is a shared, but relatively delayed, response to proteasome inhibition. However, activation of hsp27 through mitogen-activated protein kinase-dependent phosphorylation of Ser<sup>82</sup> (40) was only observed in RPMI 8226 cells.

The accumulation of cyclin B1 and p21 in HT-29 cells is consistent with the initial cell cycle arrest observed in these cells. However, in RPMI 8226 cells, the accumulation of p21 is apparently insufficient to maintain a growth arrest, presumably due to stabilization of other proteins and activation of dominant proapoptotic pathways. The precise mechanistic differences responsible for the greater sensitivity to proteasome inhibition and more rapid apoptotic induction seen in the hematologic tumor cell lines relative to solid tumor cell lines remain to be established.

**Prolonged exposure to PR-171 or bortezomib increases cytotoxicity.** Extending PR-171 and bortezomib treatment from 1 to 72 h (conditions that would be difficult to replicate *in vivo* due to

their rapid clearance) resulted in greater cytotoxicity for both compounds and eliminated the differentials between the two molecules and between the different cell types (Table 2). Extended treatment with bortezomib or PR-171 has also been shown to have potent antiproliferative and proapoptotic effects on primary human acute myeloid leukemia cells (41). Suppression of proteasome activity recovery could be responsible for the increases in cytotoxicity observed with extended exposure. Alternatively, because both PR-171 and bortezomib are covalent inhibitors, a time-dependent increase in the degree of proteasome inhibition could contribute to greater cytotoxicity. We have found that extending the length of compound exposure from 1 to 6 h results in greater total proteasome inhibition with both compounds, particularly on the trypsin-like and caspase-like active sites.<sup>1</sup> The inhibition of multiple proteasome active sites suppresses total cellular protein turnover to a greater extent than inhibition of the chymotrypsin-like site alone (29) and may therefore result in greater cytotoxicity.

**PR-171 is cleared rapidly but promotes a widespread pharmacodynamic response in rodents.** In rats, PR-171 was rapidly cleared from the plasma compartment following *i.v.* administration. Noncompartmental analysis of PR-171 pharmacokinetics revealed an average terminal plasma half-life of  $\sim 15$  min. The estimated steady-state volume of distribution was much larger than blood volume, suggesting extensive penetration of PR-171 into peripheral tissues. To determine the pharmacodynamics of PR-171, blood and tissues isolated from rats 1 h after drug administration were analyzed for proteasome chymotrypsin-like activity. PR-171 induced a dose-dependent suppression of activity in all tissues examined except the brain (Fig. 3A), suggesting that despite rapid entry into cells, the compound does not readily cross the blood-brain barrier. Liver was relatively insensitive to the pharmacodynamic effects of PR-171 perhaps due to the competition between drug metabolism and target binding. As expected, the same tissues

**Table 1.** Selective inhibition of the proteasome chymotrypsin-like activity by PR-171

Active site Inhibitory parameter	Chymotrypsin-like				Caspase-like			Trypsin-like		
	$k_{inact}/K_i$ ( $M^{-1} s^{-1}$ )	1 h IC <sub>50</sub> (nmol/L)			$k_{inact}/K_i$ ( $M^{-1} s^{-1}$ )	1 h IC <sub>50</sub> (nmol/L)		$k_{inact}/K_i$ ( $M^{-1} s^{-1}$ )	1 h IC <sub>50</sub> (nmol/L)	
Proteasome preparation	20S	20S	Cell lysate	Immuno 20S	20S	20S	Cell lysate	20S	20S	Cell lysate
Inhibitor										
PR-171	33,000	6 ± 2	4 ± 2	33 ± 17	<100*	2,400 ± 500	1,000 ± 550	<100*	3,600 ± 850	1,100 ± 470
Bortezomib	38,000	7 ± 2	6 ± 1	4 ± 2	5,700	74 ± 36	55 ± 22	<100*	4,200 ± 1,900	600 ± 190
<i>Clasto</i> -lactacystin β-lactone	ND	62 ± 18	37 ± 24	440 ± 180	ND	14,000 ± 9,000	4,200 ± 1,500	ND	2,000 ± 700	860 ± 200
Salinosporamide A <sup>†</sup>	ND	3.5 ± 0.3	ND	ND	ND	430 ± 34	ND	ND	28 ± 2	ND

NOTE: Proteasome activity was measured spectrofluorometrically by monitoring the hydrolysis of Leu-Leu-Val-Tyr-AMC (chymotrypsin-like), Leu-Leu-Glu-AMC (caspase-like) and Leu-Arg-Arg-AMC (trypsin-like) substrates. Values reported are the mean ± SD from ≥4 determinations.

Abbreviation: ND, not determined.

\*<100: Inhibition kinetics were too slow to determine  $k_{inact}/K_i$  values at inhibitor concentrations as high as 10 μmol/L.

† IC<sub>50</sub> values for salinosporamide A from Chauhan et al. (20).

that showed chymotrypsin-like inhibition also showed extensive penetration by [<sup>3</sup>H]-PR-171 (Fig. 3B). A similarly rapid clearance (19) and widespread tissue distribution (33, 42) has been reported for bortezomib. Although the pharmacokinetics and tissue pharmacodynamics of salinosporamide A have not been thoroughly characterized, its instability in aqueous environments (42) is likely to result in brief exposure in animals as well. Unlike PR-171 and bortezomib, i.v. administered salinosporamide A inhibits proteasome activity in the brain (42).

The *in vivo* proteasome active site selectivities of PR-171 and bortezomib were examined in mice 1 h after i.v. drug administration (Fig. 3C). At doses that induced >80% inhibition of chymotrypsin-like activity in blood, bortezomib, but not PR-171, was able to mediate pronounced inhibition of the caspase-like

activity. Neither compound had significant activity on the trypsin-like activity. These results are consistent with the active site selectivity profiles observed in cells (Fig. 1B). Chauhan et al. (20) have reported similar results with bortezomib and have also shown that salinosporamide A, at a dose that fully inhibits proteasome chymotrypsin-like activity in blood, can also partially suppress the trypsin-like and caspase-like activities.

**Proteasome activity recovers in tissues following PR-171 administration.** To evaluate the recovery of proteasome activity in animals, tissues were examined at varying time points after i.v. PR-171 administration. With the exception of whole blood, proteasome activity recovered by 50% to 100% within 24 h following PR-171 dosing in all tissues examined in both mice (Fig. 3D) and rats (Supplementary Fig. S2 and data not shown). In whole blood,

**Table 2.** Cytotoxicity profiles of PR-171 and bortezomib

Cell type	Cell line	Origin	Cell viability IC <sub>50</sub> (nmol/L) 1 h treatment/72 h washout		Cell viability IC <sub>50</sub> (nmol/L) 72 h treatment	
			PR-171	Bortezomib	PR-171	Bortezomib
Hematologic tumor	RPMI 8226	Multiple myeloma	71 ± 22	303 ± 52	10 ± 3.3	4.5 ± 2.5
	HS-Sultan	B-cell lymphoma (Burkitt's)	135 ± 30	454 ± 60	5.2 ± 2.3	5.4 ± 2.0
	Molt4	Acute lymphoblastic leukemia	31 ± 17	126 ± 52	3.1 ± 1.6	6.2 ± 2.7
	RL	B cell lymphoma (NHL)	164 ± 92	814 ± 476	2.4 ± 0.4	3.4 ± 2.0
Solid tumor	HT-29	Colorectal adenocarcinoma	350 ± 84	2,190 ± 390	6.2 ± 3.9	5.0 ± 2.6
	MiaPaCa-2	Pancreatic carcinoma	1,110 ± 240	>6,500	8.9 ± 6.5	8.3 ± 2.3
	A549	Lung carcinoma	1,200 ± 900	4,600 ± 1,900	20 ± 8	13 ± 8
Nontransformed	NHDF	Normal skin	389 ± 128	2,460 ± 1,120	14 ± 4.5	6.3 ± 4.1
	HUVEC	Normal umbilical vein	455 ± 45	3,510 ± 390	7.2 ± 1.3	3.5 ± 0.5

NOTE: Cell viability was measured with CellTiter-Glo reagent either after continuous compound exposure for 72 h or with 1 h compound exposure followed by a 72 h washout period. Values reported are the mean ± SD from ≥3 determinations.

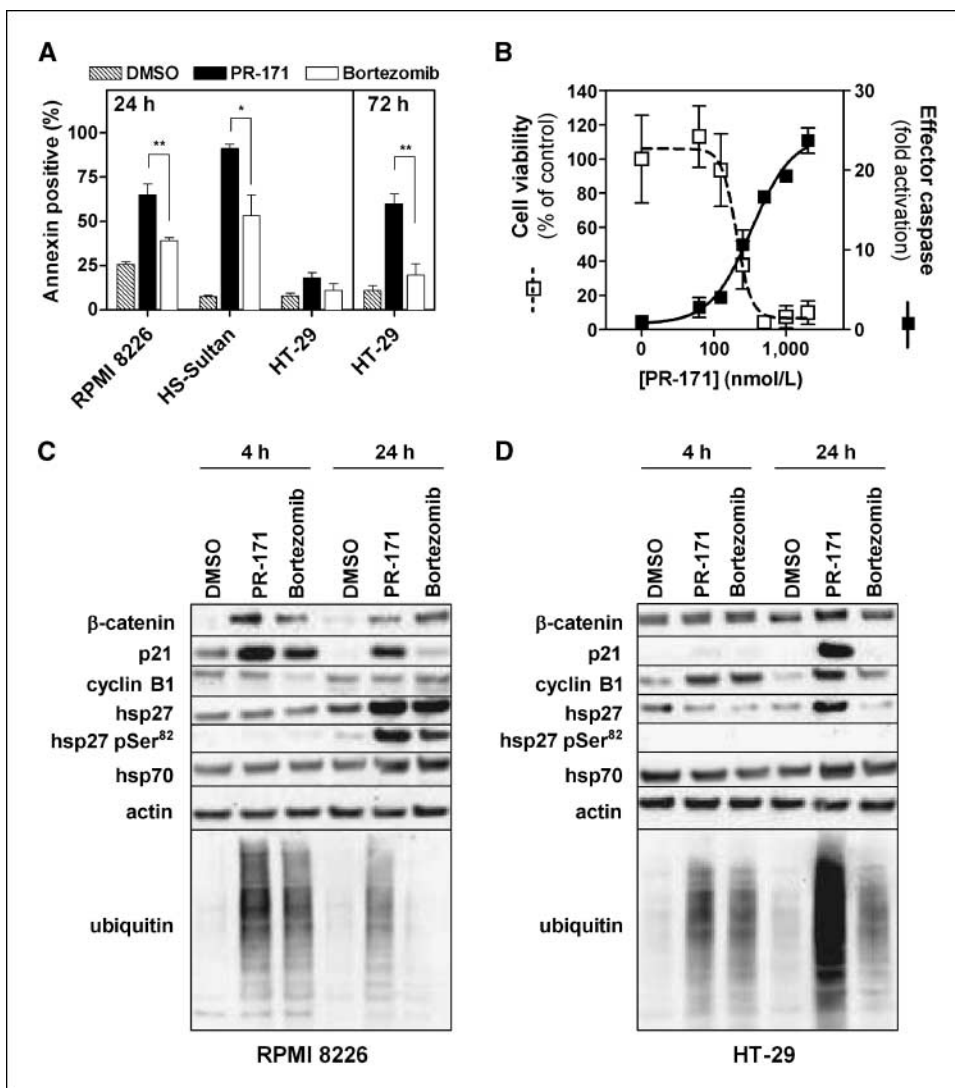


**Figure 2.** Induction of apoptosis and marker accumulation. **A**, apoptosis of tumor cell lines following brief exposure to PR-171 or bortezomib. Tumor cell lines were treated with PR-171 (solid columns) or bortezomib (open columns) for 1 h at a concentration of either 500 nmol/L (RPMI 8226 and HS-Sultan) or 2 μmol/L (HT-29 cells). Vehicle consisted of 0.25% DMSO (hatched columns). Cells were harvested at 24 h (all cell lines) and 72 h (HT-29 only) following treatment and analyzed for apoptosis by cell surface annexin V staining. Columns, mean from three experiments; bars, SD. \*,  $P < 0.05$ ; \*\*,  $P < 0.01$ . **B**, effector caspase activation in HS-Sultan following brief exposure to PR-171. HS-Sultan cells were treated with a range of PR-171 concentrations for 1 h. Effector caspase activity (caspase 3/7; ■) was measured 5 h after compound washout and is expressed as fold activation relative to cells treated with 0.25% DMSO. For comparison, cell viability (□) was measured 24 h after compound washout and is expressed as the percent relative to cells treated with 0.25% DMSO. **C** and **D**, stabilization and accumulation of markers in tumor cell lines following brief exposure to proteasome inhibitors. Lysates were prepared from RPMI 8226 (**C**) or HT-29 (**D**) cells 4 and 24 h following a 1-h treatment with 0.25% DMSO, PR-171, or bortezomib (500 nmol/L for RPMI 8226 and 2 μmol/L for HT-29). Western blot analysis was done with antibodies generated against β-catenin, p21, cyclin B1, hsp27, hsp27 phospho-Ser<sup>82</sup>, hsp70, and ubiquitin. Actin was used to verify the uniformity of gel loading.

a much slower rate of proteasome activity recovery was observed following PR-171 treatment (<50% recovery after 1 week), highlighting the impact of an irreversible mechanism of action in a cell type (erythrocytes) that cannot recover activity by making new proteasomes. Salinosporamide A, due to its irreversible mechanism (43), also induces proteasome inhibition in blood that recovers slowly (20). In contrast, complete recovery of proteasome activity in blood was achieved by 48 h following bortezomib dosing (Fig. 3D and ref. 20) due to its slowly reversible mechanism of action. In tissues, recovery from bortezomib-mediated inhibition was comparable to PR-171 ( $t_{1/2} \sim 24$  h), but faster than blood recovery, suggesting that new proteasome synthesis, and not the slow reversibility of bortezomib, plays a dominant role in proteasome activity recovery in tissues other than whole blood.

In rats, proteasome inhibition and recovery was also examined following two (QDx2) or five (QDx5) consecutive daily doses of PR-171 (Supplementary Fig. S2). There were no significant differences in either the level of inhibition or rate of recovery of chymotrypsin-like activity in bone marrow following QDx2 dosing or QDx5 dosing as compared with a single dose. In contrast, a cumulative inhibition of chymotrypsin-like activity was evident in blood following QDx2 dosing which was even more pronounced

following QDx5 dosing of PR-171. This cumulative inhibition is likely due to the inability of erythrocytes to recover activity between doses.

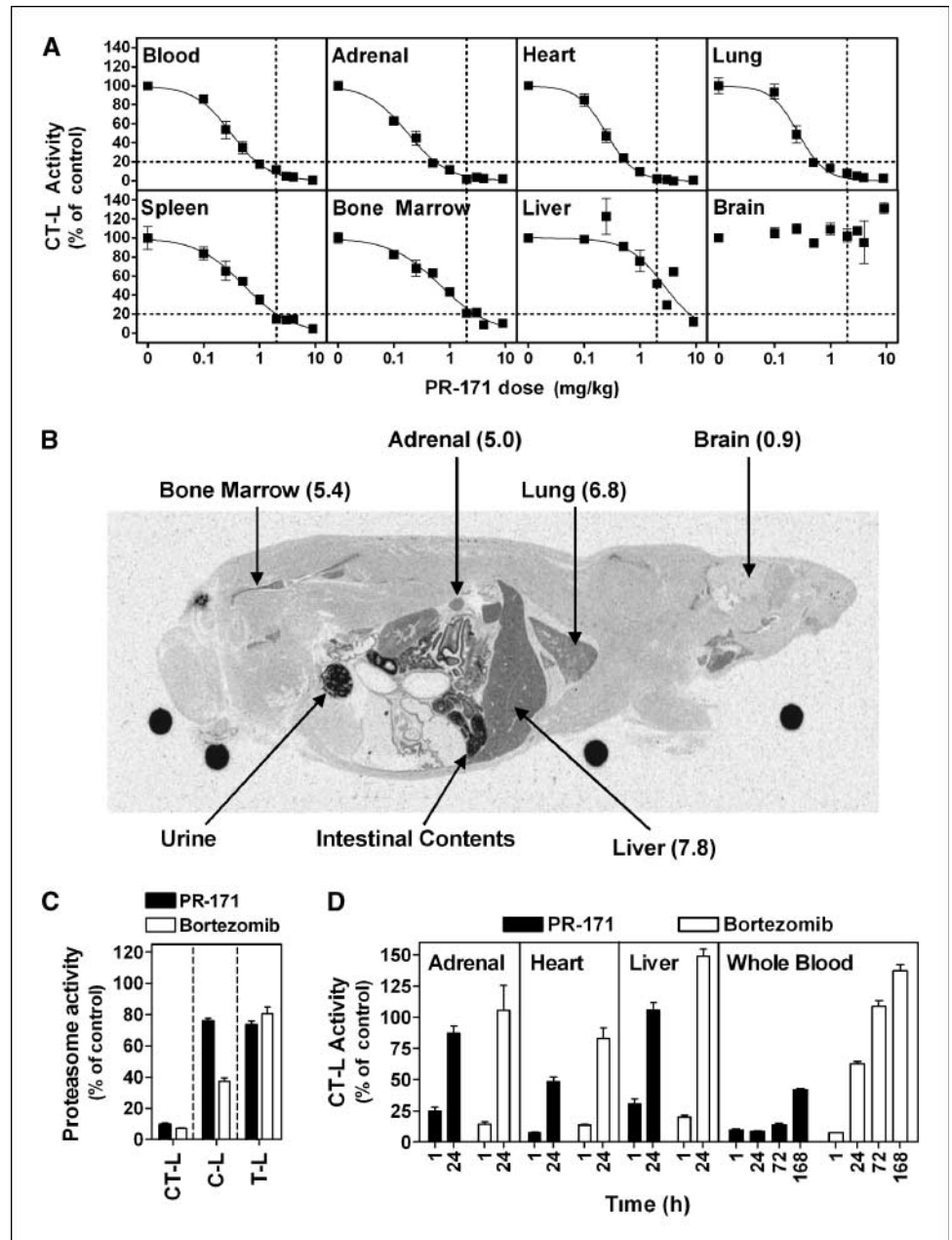
**Daily dosing of PR-171 is well tolerated.** Despite the sustained proteasome inhibition in erythrocytes and repeated suppression of proteasome activity in other tissues achieved with the QDx5 schedule, no changes in hematocrit or hemoglobin concentration were observed, and no significant weight loss was noted in animals at doses up to 2 mg/kg (data not shown). These results show that repeated administration of PR-171 in rodents for up to 5 consecutive days is well tolerated even at doses resulting in peak inhibition of the proteasome chymotrypsin-like activity in excess of 80% in blood and most other tissues (see Fig. 3A). Daily dosing schedules that prevent full recovery of proteasome activity between doses and are more intensive than the recommended clinical dosing schedule for bortezomib and the preclinical dosing schedule tested with salinosporamide A (biweekly day 1/day 4; refs. 8, 18, 20). As noted above, it is possible that the greater biochemical selectivity of PR-171 for the chymotrypsin-like activity of the proteasome may contribute to greater tolerability *in vivo*. Other factors, including biodistribution differences, could also contribute to distinct safety profiles for the various proteasome inhibitors.

**Intensive PR-171 dosing results in improved antitumor efficacy in human tumor xenograft models.** The antitumor activity of PR-171 was evaluated and compared with bortezomib in BNX mice bearing established human tumor xenografts derived from three tumor cell lines: HT-29 (colorectal adenocarcinoma; Fig. 4A), RL (B cell lymphoma; Fig. 4B), and HS-Sultan (Burkitt's lymphoma; Fig. 4C). All PR-171 dosing schedules (up to 5 mg/kg delivered weekly QDx2) were tolerated in the tumor-bearing animals, resulting in weight loss of <10% (data not shown). The bortezomib dose (1 mg/kg on a biweekly day 1/day 4 schedule) was determined to be the maximum tolerated dose in this mouse strain (see also ref. 44). In all three models, 5 mg/kg PR-171 delivered i.v. on a weekly QDx2 schedule was more efficacious than 1 mg/kg bortezomib delivered i.v. on its standard clinical schedule (biweekly day 1/day 4). When the same 5 mg/kg dose of PR-171 was given on a day 1/day 4 schedule or combined into a single weekly 10 mg/kg

dose, efficacy was eliminated in the HT-29 model. In addition, lowering the PR-171 dose to 3 mg/kg on the weekly QDx2 schedule reduced efficacy in both the RL and HS-Sultan models. These results show that the activity of PR-171 is dose and schedule dependent. Both bortezomib and salinosporamide A are efficacious in other xenograft models, including multiple myeloma models (20, 21, 33, 44), but neither has been tested with a weekly QDx2 dosing schedule.

At the doses used in our efficacy studies, both PR-171 and bortezomib suppressed proteasome activity in blood and adrenals to an equivalent extent (Fig. 4D). This suggests that the improved antitumor activity of PR-171 delivered on the weekly QDx2 schedule (relative to biweekly day 1/day 4 dosing of either PR-171 or bortezomib) may be due to suppression of proteasome activity recovery between doses. Antitumor efficacy was achieved with PR-171 despite the fact that proteasome activity was inhibited

**Figure 3.** Systemic proteasome inhibition following i.v. administration of PR-171. **A**, inhibition of proteasome activity in rat tissues. Proteasome chymotrypsin-like (CT-L) activity was measured by Leu-Leu-Val-Tyr-AMC hydrolysis in lysates prepared from whole blood, erythrocyte-depleted bone marrow, splenocytes, liver, lung, brain, heart, and adrenal 1 h following i.v. administration of PR-171 at doses ranging from 0.1 to 9 mg/kg. Data are presented as the mean activity relative to vehicle controls ( $\pm$  SE;  $n = 3-6$  per dose group). Horizontal and vertical dotted lines, 80% proteasome inhibition and 2 mg/kg dose level, respectively. **B**, distribution of radiolabeled PR-171 in rats. Whole body autoradiography was done 0.5 h after i.v. administration of 2 mg/kg [ $^3$ H]-PR-171 to rats. Numbers in parentheses, nanogram equivalents of [ $^3$ H]-PR-171 per milligram of tissue. Low exposure to [ $^3$ H]-PR-171 was also noted in testis (data not shown), similar to the distribution reported for radiolabeled bortezomib (33). **C**, proteasome active site selectivity in mouse blood. Proteasome chymotrypsin-like, caspase-like (C-L), and trypsin-like (T-L) activities were measured in mouse blood lysates by Leu-Leu-Val-Tyr-AMC, Leu-Leu-Glu-AMC, and Leu-Arg-Arg-AMC, respectively. Blood samples were collected 1 h following administration of PR-171 (5 mg/kg; solid columns) or bortezomib (1 mg/kg; open columns). Columns, mean activity relative to vehicle controls; bars, SE ( $n = 3$  per dose group). **D**, proteasome inhibition and recovery following a single dose of PR-171 or bortezomib in mouse. BALB/c mice received a single i.v. dose of PR-171 (5 mg/kg; solid columns) or bortezomib (1 mg/kg; open columns) and proteasome chymotrypsin-like activity was measured in lysates prepared from tissues or whole blood at 1- and 24-h time points. For whole blood, chymotrypsin-like activity was also measured 72 h and 7 d following drug administration. Columns, mean activity relative to vehicle controls; bars, SE ( $n = 3$  per dose group).



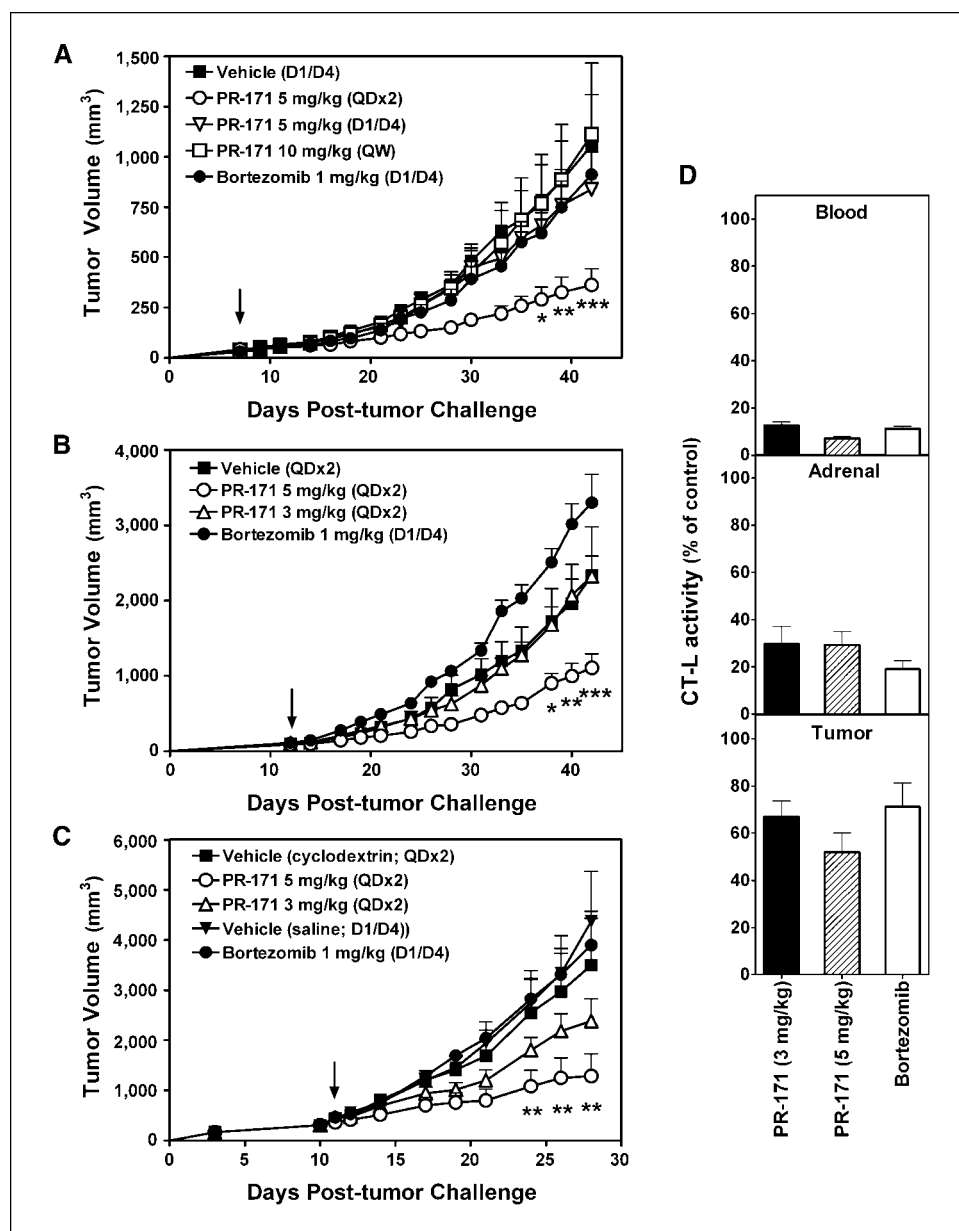


**Figure 4.** Antitumor efficacy of PR-171 in mice bearing human tumor xenografts. **A**, schedule-dependent efficacy of PR-171 in HT-29 colorectal adenocarcinoma xenograft model. BNX mice (females,  $n = 7$  per group) bearing established ( $\sim 50 \text{ mm}^3$ ) s.c. tumors were randomized on day 7 ( $\downarrow$ ) into treatment groups receiving biweekly administration of cyclodextrin/citrate vehicle ( $\blacksquare$ ), 1 mg/kg bortezomib ( $\bullet$ ) or 5 mg/kg PR-171 ( $\nabla$ ) on days 1 and 4, biweekly administration of 5 mg/kg PR-171 on days 1 and 2 ( $\circ$ ), or weekly administration of 10 mg/kg PR-171 on day 1 ( $\square$ ). All treatments were given as i.v. bolus administrations, and treatment lasted for 3 wks. Tumor volumes were measured thrice per week and are presented as mean tumor volume  $\pm$  SE. \*,  $P < 0.05$ ; \*\*,  $P < 0.01$ ; \*\*\*,  $P < 0.001$ . Data presented are from one of two experiments with similar results. **B**, dose-dependent efficacy of PR-171 in RL lymphoma xenograft model. BNX mice (females  $n = 7$  per group) bearing established ( $\sim 90 \text{ mm}^3$ ) s.c. RL tumors were randomized on day 12 ( $\downarrow$ ) into treatment groups receiving biweekly administration of cyclodextrin/citrate vehicle ( $\blacksquare$ ), 3 mg/kg PR-171 ( $\triangle$ ), or 5 mg/kg PR-171 ( $\circ$ ) on days 1 and 2 or biweekly administration of 1 mg/kg bortezomib ( $\bullet$ ) on days 1 and 4. All treatments were given as i.v. bolus administrations, and treatment lasted for 2 wks. Tumor volumes were measured thrice per week and are presented as mean tumor volume  $\pm$  SE. \*,  $P < 0.05$ ; \*\*,  $P < 0.01$ ; and \*\*\*,  $P < 0.001$ . Data presented are from one of two experiments with similar results. **C**, dose-dependent efficacy of PR-171 in HS-Sultan lymphoma xenograft model. BNX mice (females  $n = 7$  per group) bearing established ( $\sim 300 \text{ mm}^3$ ) s.c. HS-Sultan tumors were randomized on day 11 ( $\downarrow$ ) into treatment groups receiving biweekly administration of cyclodextrin/citrate vehicle ( $\blacksquare$ ), 3 mg/kg PR-171 ( $\triangle$ ), or 5 mg/kg PR-171 ( $\circ$ ) on days 1 and 2 or biweekly administration of saline vehicle ( $\blacktriangledown$ ) or 1 mg/kg bortezomib ( $\bullet$ ) on days 1 and 4. All treatments were given as i.v. bolus administrations, and treatment lasted for 2 wks. Tumor volumes were measured thrice per week and are presented as mean tumor volume  $\pm$  SE. \*\*,  $P < 0.01$ . Data presented are from one of two experiments with similar results. **D**, tissue and tumor pharmacodynamics. Proteasome chymotrypsin-like activity was measured in whole blood, adrenals, and HS-Sultan tumor 1 h after a single dose of 3 mg/kg (solid columns) or 5 mg/kg (hatched columns) PR-171 or 1 mg/kg bortezomib (open columns). Columns, mean activity relative to vehicle controls; bars, SE ( $n = 6$  per dose group from two independent experiments).

in HS-Sultan tumors to a lesser extent than other tissues (Fig. 4D). Similar observations of low tumor proteasome inhibition have been reported with both bortezomib (33, 44) and salinosporamide A (42). This raises the possibility that mechanisms other than direct

cytotoxicity to the tumor cells may contribute to antitumor efficacy. One such mechanism could be an antiangiogenic activity, as has been observed with bortezomib (13). Alternative explanations for the low tumor pharmacodynamic response at efficacious



doses include enhanced sensitivity of the tumor cells *in vivo* to proteasome inhibition or high local proteasome inhibition within critical subdomains of the tumor (due to heterogeneous penetration by the drug; ref. 45).

Taken together, the results described in the present study show that the novel proteasome inhibitor PR-171 has several *in vitro* and *in vivo* properties that distinguish it from bortezomib and salinosporamide A. Most importantly, PR-171 can be delivered with intensive daily dosing schedules that inhibit proteasome activity by >80% in most tissues without excessive toxicity. Furthermore, our xenograft studies show that more intensive dosing schedules can yield greater efficacy in both solid and hematologic tumor models. Supported by the preclinical

results presented here, two phase I clinical trials in multiple myeloma and NHL patients have been initiated with PR-171 comparing two dose-intensive schedules (QDx2 and QDx5). The extent to which the distinct *in vitro* and *in vivo* properties of PR-171, salinosporamide A, and bortezomib impact clinical efficacy or safety will be determined in these ongoing or upcoming trials.

## Acknowledgments

Received 11/7/2006; revised 3/30/2007; accepted 5/2/2007.

The costs of publication of this article were defrayed in part by the payment of page charges. This article must therefore be hereby marked *advertisement* in accordance with 18 U.S.C. Section 1734 solely to indicate this fact.

## References

- Ciechanover A. Proteolysis: from the lysosome to ubiquitin and the proteasome. *Nat Rev Mol Cell Biol* 2005;6:79–87.
- Dalton WS. The proteasome. *Semin Oncol* 2004;31:3–9.
- Kisselev AF, Goldberg AL. Proteasome inhibitors: from research tools to drug candidates. *Chem Biol* 2001;8:739–58.
- Adams J. The proteasome: a suitable antineoplastic target. *Nat Rev Cancer* 2004;4:349–60.
- Kisselev AF, Goldberg AL. Monitoring activity and inhibition of 26S proteasomes with fluorogenic peptide substrates. *Methods Enzymol* 2005;398:364–78.
- Chauhan D, Hideshima T, Mitsiades C, Richardson P, Anderson KC. Proteasome inhibitor therapy in multiple myeloma. *Mol Cancer Ther* 2005;4:686–92.
- Adams J, Behnke M, Chen S, et al. Potent and selective inhibitors of the proteasome: dipeptidyl boronic acids. *Bioorg Med Chem Lett* 1998;8:333–8.
- Richardson PG, Sonneveld P, Schuster MW, et al. Bortezomib or high-dose dexamethasone for relapsed multiple myeloma. *N Engl J Med* 2005;352:2487–98.
- Goy A, Younes A, McLaughlin P, et al. Phase II study of proteasome inhibitor bortezomib in relapsed or refractory B-cell non-Hodgkin's lymphoma. *J Clin Oncol* 2005; 23:667–75.
- O'Connor OA, Wright J, Moskowitz C, et al. Phase II clinical experience with the novel proteasome inhibitor bortezomib in patients with indolent non-Hodgkin's lymphoma and mantle cell lymphoma. *J Clin Oncol* 2005;23:676–84.
- Hideshima T, Chauhan D, Richardson P, et al. NF- $\kappa$ B as a therapeutic target in multiple myeloma. *J Biol Chem* 2002;277:16639–47.
- Hideshima T, Richardson P, Chauhan D, et al. The proteasome inhibitor PS-341 inhibits growth, induces apoptosis, and overcomes drug resistance in human multiple myeloma cells. *Cancer Res* 2001;61:3071–6.
- Roccaro AM, Hideshima T, Raje N, et al. Bortezomib mediates antiangiogenesis in multiple myeloma via direct and indirect effects on endothelial cells. *Cancer Res* 2006;66:184–91.
- Lee AH, Iwakoshi NN, Anderson KC, Glimcher LH. Proteasome inhibitors disrupt the unfolded protein response in myeloma cells. *Proc Natl Acad Sci U S A* 2003;100:9946–51.
- Obeng EA, Carlson LM, Gutman DM, Harrington WJ, Jr., Lee KP, Boise LH. Proteasome inhibitors induce a terminal unfolded protein response in multiple myeloma cells. *Blood* 2006;107:4907–16.
- Richardson PG, Briemberg H, Jagannath S, et al. Frequency, characteristics, and reversibility of peripheral neuropathy during treatment of advanced multiple myeloma with bortezomib. *J Clin Oncol* 2006;24:3113–20.
- Lonial S, Waller EK, Richardson PG, et al. Risk factors and kinetics of thrombocytopenia associated with bortezomib for relapsed, refractory multiple myeloma. *Blood* 2005;106:3777–84.
- Orlowski RZ, Stinchcombe TE, Mitchell BS, et al. Phase I trial of the proteasome inhibitor PS-341 in patients with refractory hematologic malignancies. *J Clin Oncol* 2002;20:4420–7.
- Papandreou CN, Daliani DD, Nix D, et al. Phase I trial of the proteasome inhibitor bortezomib in patients with advanced solid tumors with observations in androgen-independent prostate cancer. *J Clin Oncol* 2004;22:2108–21.
- Chauhan D, Catley L, Li G, et al. A novel orally active proteasome inhibitor induces apoptosis in multiple myeloma cells with mechanisms distinct from Bortezomib. *Cancer Cell* 2005;8:407–19.
- Cusack JC, Jr., Liu R, Xia L, et al. NPI-0052 enhances tumoricidal response to conventional cancer therapy in a colon cancer model. *Clin Cancer Res* 2006;12:6758–64.
- Macherla VR, Mitchell SS, Manam RR, et al. Structure-activity relationship studies of salinosporamide A (NPI-0052), a novel marine derived proteasome inhibitor. *J Med Chem* 2005;48:3684–7.
- Hanada M, Sugawara K, Kaneta K, et al. Epoxomicin, a new antitumor agent of microbial origin. *J Antibiot (Tokyo)* 1992;45:1746–52.
- Sin N, Kim KB, Eloffson M, et al. Total synthesis of the potent proteasome inhibitor epoxomicin: a useful tool for understanding proteasome biology. *Bioorg Med Chem Lett* 1999;9:2283–8.
- Groll M, Kim KB, Kairies N, Huber R, Crews CM. Crystal structure of epoxomicin:20S proteasome reveals a molecular basis of  $\alpha'$ , $\beta'$ -epoxyketone proteasome inhibitors. *J Am Chem Soc* 2000;122:1237–8.
- Eloffson M, Splittgerber U, Myung J, Mohan R, Crews CM. Towards subunit-specific proteasome inhibitors: synthesis and evaluation of peptide  $\alpha'$ , $\beta'$ -epoxyketones. *Chem Biol* 1999;6:811–22.
- Smyth MS, Laidig GJ. Compounds for enzyme inhibition. US patent application US 2006/0030533 A1.
- Groettrup M, van den BM, Schwarz K, et al. Structural plasticity of the proteasome and its function in antigen processing. *Crit Rev Immunol* 2001;21:339–58.
- Kisselev AF, Callard A, Goldberg AL. Importance of the different proteolytic sites of the proteasome and the efficacy of inhibitors varies with the protein substrate. *J Biol Chem* 2006;281:8582–90.
- Groll M, Berkers CR, Ploegh HL, Ova H. Crystal structure of the boronic acid-based proteasome inhibitor bortezomib in complex with the yeast 20S proteasome. *Structure* 2006;14:451–6.
- Mitsiades N, Mitsiades CS, Poulaki V, et al. Molecular sequelae of proteasome inhibition in human multiple myeloma cells. *Proc Natl Acad Sci U S A* 2002;99:14374–9.
- Meiners S, Heyken D, Weller A, et al. Inhibition of proteasome activity induces concerted expression of proteasome genes and *de novo* formation of mammalian proteasomes. *J Biol Chem* 2003;278: 21517–25.
- Adams J, Palombella VJ, Sausville EA, et al. Proteasome inhibitors: a novel class of potent and effective antitumor agents. *Cancer Res* 1999;59:2615–22.
- Aberle H, Bauer A, Stappert J, Kispert A, Kemler R.  $\beta$ -catenin is a target for the ubiquitin-proteasome pathway. *EMBO J* 1997;16:3797–804.
- Ling YH, Liebes L, Jiang JD, et al. Mechanisms of proteasome inhibitor PS-341-induced G<sub>2</sub>/M-phase arrest and apoptosis in human non-small cell lung cancer cell lines. *Clin Cancer Res* 2003;9:1145–54.
- Ito H, Kamei K, Iwamoto I, et al. Inhibition of proteasomes induces accumulation, phosphorylation, and recruitment of HSP27 and  $\alpha$ B-crystallin to aggregates. *J Biochem Tokyo* 2002;131:593–603.
- Ling YH, Liebes L, Ng B, et al. PS-341, a novel proteasome inhibitor, induces Bcl-2 phosphorylation and cleavage in association with G<sub>2</sub>/M phase arrest and apoptosis. *Mol Cancer Ther* 2002;1:841–9.
- Chauhan D, Li G, Shringarpure R, et al. Blockade of Hsp27 overcomes bortezomib/proteasome inhibitor PS-341 resistance in lymphoma cells. *Cancer Res* 2003;63: 6174–7.
- Bush KT, Goldberg AL, Nigam SK. Proteasome inhibition leads to a heat-shock response, induction of endoplasmic reticulum chaperones, and thermotolerance. *J Biol Chem* 1997;272:9086–92.
- Rogalla T, Ehrnsperger M, Preville X, et al. Regulation of Hsp27 oligomerization, chaperone function, and protective activity against oxidative stress/tumor necrosis factor  $\alpha$  by phosphorylation. *J Biol Chem* 1999;274: 18947–56.
- Stapnes C, Doskeland AP, Hatfield K, et al. The proteasome inhibitors bortezomib and PR-171 have antiproliferative and proapoptotic effects on primary human acute myeloid leukaemia cells. *Br J Haematol* 2007;136:814–28.
- Williamson MJ, Blank JL, Bruzzese FJ, et al. Comparison of biochemical and biological effects of ML858 (salinosporamide A) and bortezomib. *Mol Cancer Ther* 2006;5:3052–61.
- Groll M, Huber R, Potts BC. Crystal structures of Salinosporamide A (NPI-0052) and B (NPI-0047) in complex with the 20S proteasome reveal important consequences of  $\beta$ -lactone ring opening and a mechanism for irreversible binding. *J Am Chem Soc* 2006;128: 5136–41.
- LeBlanc R, Catley LP, Hideshima T, et al. Proteasome inhibitor PS-341 inhibits human myeloma cell growth *in vivo* and prolongs survival in a murine model. *Cancer Res* 2002;62:4996–5000.
- Au JL, Jang SH, Zheng J, et al. Determinants of drug delivery and transport to solid tumors. *J Control Release* 2001;74:31–46.